



ELSEVIER

Contents lists available at SciVerse ScienceDirect

European Polymer Journal

journal homepage: www.elsevier.com/locate/europolj

New optical limiting polymeric materials with different π -electron conjugation bridge structures: Synthesis and characterization

K.A. Vishnumurthy, M.S. Sunitha, A. Vasudeva Adhikari*

Department of Chemistry, National Institute of Technology Karnataka, Surathkal, Mangalore 575025, India

ARTICLE INFO

Article history:

Received 3 October 2011

Received in revised form 2 June 2012

Accepted 7 June 2012

Available online 28 June 2012

Keywords:

3,4-Dialkoxythiophene

Cyanopyridine

Optical limiting

NLO

ABSTRACT

In this communication we describe the design and synthesis of five new conjugated polymers (**P1–P5**) with various π -electron conjugation bridges. Their structures were established by FTIR, ^1H NMR spectroscopy, elemental analysis. The molecular weights of the polymers were estimated by gel permeation chromatographic technique. Further, their electrochemical, linear and nonlinear optical properties were investigated. The electrochemical band gaps of **P1–P5** were found to be 1.72–2.35 eV. Their third-order nonlinear optical activities were studied by open aperture Z-scan technique, using a Q-switched, frequency doubled Nd:YAG laser producing 7 nano second laser pulses at 532 nm. Z-scan results reveal that the polymers exhibit self-defocusing nonlinearity and their operating mechanism involves reverse saturable absorption. The polymers showed strong optical limiting behavior due to effective two-photon absorption (2PA) with 2PA coefficients of the order of 10^{-11} m/W, which is comparable to that of good optical limiting materials in the literature.

© 2012 Elsevier Ltd. All rights reserved.

1. Introduction

Conjugated polymeric materials exhibiting strong nonlinear optical properties with fast response time have attracted considerable interest in recent years because of their usages in optoelectronic and photonic devices. Recently the applicability of conjugated polymeric materials as optical limiters has received significant attention owing to the growing needs for protection of optically sensitive devices and human eyes from laser damage in both civilian and military applications [1,2].

Over the past decade, the field of nonlinear optics has gained considerable research interest, with most of the attention being focused on establishing the fundamental relationship between nonlinear optical response and chemical structure. In this context, a large number of inorganic and organic materials have been reported to exhibit promising NLO properties. Amongst them, π -conjugated

polymers play a significant role because of their wide range of tunable optical, structural and mechanical properties. They possess characteristically large electronic polarizabilities and hence it is reasonable to expect these molecules to possess substantial hyperpolarizabilities [3,4] as the nonlinear response of any material is a manifestation of higher orders of their molecular polarizability. In conjugated polymers the hyperpolarizability can be further enhanced by incorporating electron acceptor and electron donor units along the main chain. This concept of donor–acceptor (D–A) approach has resulted in enhancement in their optical limiting behavior [5]. Such aromatic D–A type molecules with push–pull mechanism were reported to be quite stable and were found to exhibit very good β values.

Thiophene based conjugated polymers were known to possess good NLO behavior. According to the literature, 3,4-dialkoxy thiophene based conjugated polymers exhibit low band gap, mainly due to the presence of electron donating alkoxy side chain and further, the incorporation of electron withdrawing oxadiazole ring along the conjugation path increases the charge carrying property of the

* Corresponding author. Tel.: +91 8242474046; fax: +91 8242474033.

E-mail addresses: avachem@gmail.com, avchem@nitk.ac.in (A.V. Adhikari).

polymers [6,7]. In addition to this, introduction of different electron releasing π -electron conjugation bridges such as thiophene, vinylic and naphthyl moieties brings about enhancement in the conjugation path length which in turn increases the optical limiting behavior of resulting polymers.

Cyanopyridine is an interesting molecule with very good fluorescent properties. The literature review reveals that inclusion of strong electron withdrawing cyanopyridine ring into the polymer network leads to enhancement in their optical limiting behavior [8,9]. Further, as its presence increases the conjugation path length of the polymer, the incorporation of cyanopyridine moiety lowers the band gap of the resultant molecule.

In the literature, there are several reports explaining the effect of donor–acceptor strength and conjugation length of the molecule on the optical limiting properties of aromatic organic materials [10–15]. However, no reports appeared on the study of the effect of the π -electron conjugation bridge structures, viz. naphthalene, vinylene and theinyl-vinylens on the optical limiting properties of thiophene based conjugated polymers. Theoretically, introduction of these π -electron conjugation bridge structures enhances the molecular hyperpolarizability and hence their optical limiting behavior is expected to increase.

Against this background, we have designed five new D–A type 3,4 ditetradecyloxy thiophene based conjugated polymers **P1–P5**. In present study we have introduced thiophene, naphthyl, phenyl and vinylene groups as electron donors and oxadiazole, cyanovinylene and cyanopyridine as electron acceptor molecules in the polymer chain in order to study their effect on optical limiting properties. Also, incorporation of oxadiazole moiety into the polymer backbone would minimize the steric repulsion between bulky alkoxy groups of thiophene and hence it is expected to enhance the optical limiting behavior of the polymers. The newly designed polymers have been synthesized from their monomers as per the Schemes 1 and 2. Polymers **P1–P3**, **P4** and **P5** have been synthesized via polyhydrazide, Wittig condensation and Knoevenagel condensation techniques, respectively. The required monomers have been prepared from simple thiodiglycolic acid through multistep reactions. The structures of the intermediates and corresponding polymers have been established by various spectral techniques and further, their electrochemical,

linear and nonlinear optical properties have been evaluated in order to investigate the structure–property relationship.

2. Experimental section

2.1. Materials and methods

3,4-Dialkoxythiophene-2,5-dicarboxylate **5** was synthesized according to the reported procedure [6]. All the chemicals used in present work procured from Sigma-Aldrich and Lanchester (UK). All the solvents are of analytical grade. They were purchased and used as such without any further purification.

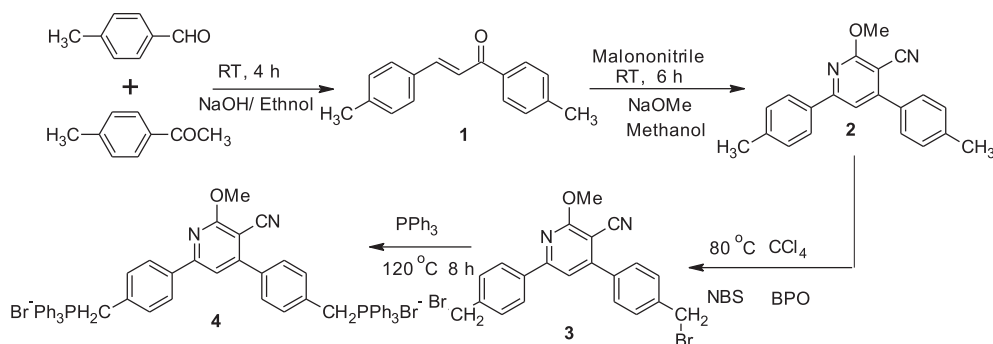
2.2. Instrumentation

Infrared spectra of all intermediate compounds and polymers were recorded on a Nicolet Avatar 5700 FTIR (Thermo Electron Corporation). The UV–Vis and fluorescence spectra were taken in GBC Cintra 101 and Perkin Elmer LS55 fluorescence spectrophotometers respectively. ^1H NMR spectra were obtained with Bruker-400 MHz FT-NMR spectrometer using TMS/solvent signal as internal reference. Elemental analyses were performed on a Flash EA1112 CHNS analyzer (Thermo Electron Corporation). Mass spectra were recorded on a Jeol SX-102 (FAB) Mass Spectrometer. The electrochemical studies were carried out using AUTOLAB PGSTAT30 electrochemical analyzer. Molecular weights of the polymers were determined by WATER's make Gel Permeation Chromatograph (GPC) against polystyrene standards with THF as an eluent.

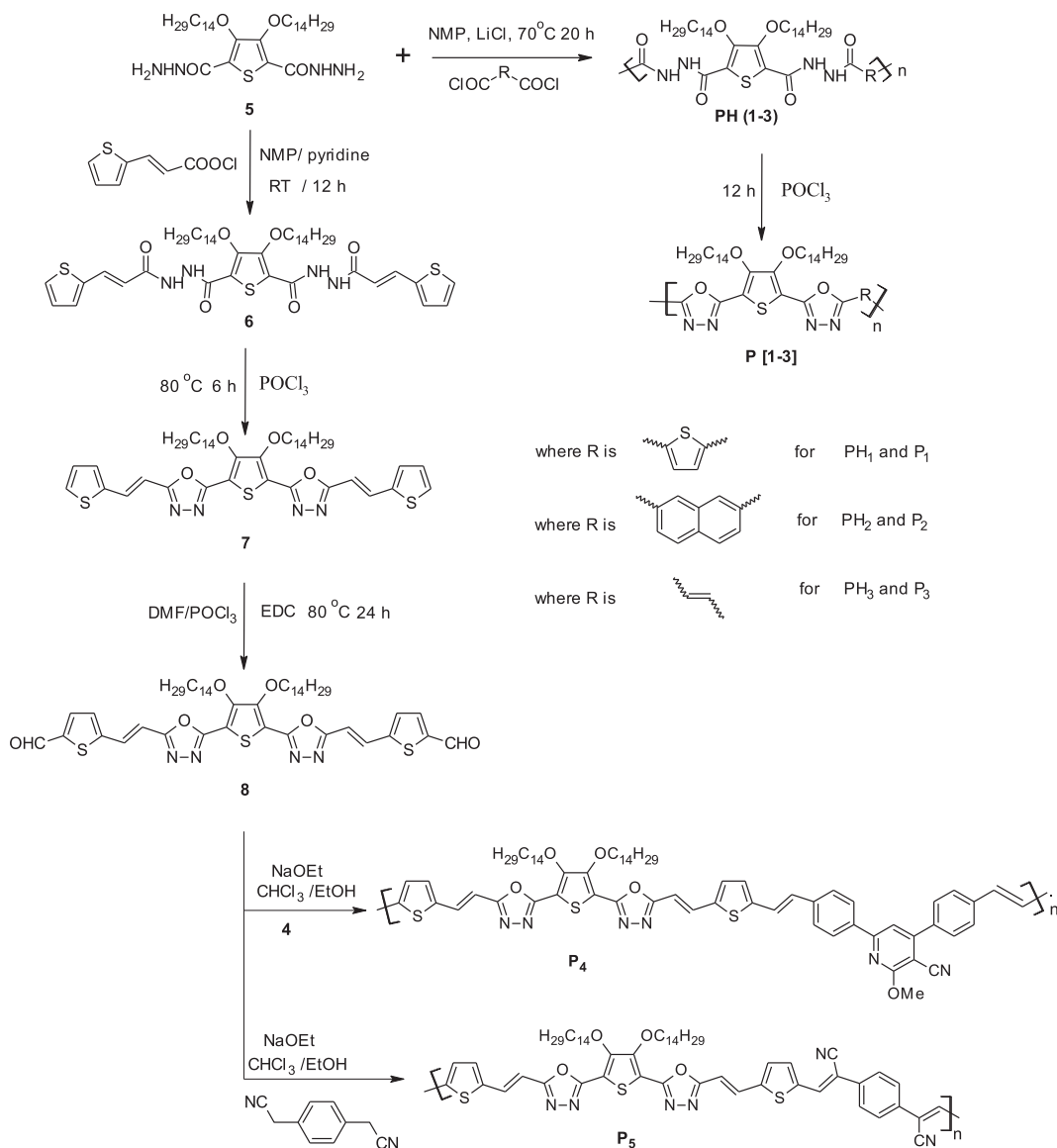
2.3. Synthesis of intermediates, monomers and polymers

2.3.1. Synthesis of 1,3-bis(4-methylphenyl)prop-2-en-1-one (**1**)

A mixture of tolualdehyde (5 g, 41.6 mmol) and 4-methylacetophenone (5.5 g, 41.6 mmol) was dissolved in 50 ml of ethanol and stirred in presence of potassium hydroxide solution (2.3 g in 5 ml water) at room temperature. After 4 h, obtained solid was filtered, and it was re-crystallized from chloroform methanol system to get yellow needle shaped solid. Yield 8.9 g (90%). FTIR (ATR, cm^{-1}): 1644,



Scheme 1. Synthesis of monomer **4**.



Scheme 2. Synthesis of monomers and polymer **P1–P5**.

1591, 1169, 987, 805, 726, *Element. Anal.* Calc. For C₁₇H₁₆O: C, 86.40; H, 6.82. Found: C, 86.41; H, 6.84%.

2.3.2. Synthesis of 2-methoxy-4,6-bis(4-methylphenyl)pyridine-3-carbonitrile (**2**)

Compound **1** (5 g, 21.1 mmol) was added slowly to a freshly prepared sodium methoxide solution (223.3 mmol of sodium in 100 mL of methanol) with constant stirring. Malononitrile (1.39 g, 21.1 mmol) was then added with continuous stirring at room temperature until the precipitate separates out. The separated solid was collected by filtration and re-crystallized from hot ethanol and chloroform. Yield: 4.5 g (67%). M.p: 142–144 °C. ¹H NMR (400 MHz, CDCl₃) δ (ppm): 8.00 (m, 2H, Ar-H), 7.55(m, 2H, Ar-H), 7.44 (s, 1H, Ar-H (pyridine)), m 7.34–7.28(m, 4H, Ar-H), 4.19 (s, 3H, –O–CH₃), 2.43 (s, 6H, Ar-CH₃), FTIR

(ATR, cm⁻¹): 2907, 2217, 1658, 1554, 1366, 1139, 818. *Element. Anal.* Calc. For C₂₁H₁₈N₂O: C, 80.23; H, 5.77; N, 8.91. Found: C, 80.25; H, 5.75; N, 8.93%.

2.3.3. Synthesis of 4,6-bis[4-(bromomethyl)phenyl]-2-methoxypyridine-3-carbonitrile (**3**)

A mixture of compound **2** (3 g, 9.5 mmol), *N*-bromosuccinimide (1.38 g, 19.1 mmol), 5 mg of benzoyl peroxide in 30 mL of carbon tetrachloride was refluxed for 8 h. After the completion of reaction, the solvent was removed under reduced pressure, 20 mL of water was added with stirring for 1 h. The resulting crude product was re-crystallized from ethyl acetate/chloroform mixture to get pure white colored solid. Yield: 3.5 g (77%). M.p.: 202–205 °C. ¹H NMR (400 MHz, CDCl₃) δ (ppm): 8.00 (m, 2H, Ar-H), 7.99–7.55(m, 4H, Ar-H), 7.5–7.3(m, 2H, Ar-H), 7.29 (s, 1H, Ar-H)

(pyridine)), 4.81 (s, 4H, Ar-CH₂-Br), 4.13 (3H, -O-CH₃), FTIR (ATR, cm⁻¹): 2993, 2219, 1580, 1546, 1359, 1139, 1007, 821,600. Element. Anal. Calc. For C₂₁H₁₆Br₂N₂O: C, 53.42; H, 3.42; N, 5.93. Found: C, 53.46; H, 3.45; N, 5.94%.

2.3.4. Synthesis of [4,6-bis[44-triphenyl phosphonium methyl phenyl]-2-methoxy, 3-cyano pyridine]dibromide (**4**)

A solution of dibromide compound **3** (1 g, 6.3 mmol) and triphenyl phosphine (3.34 g, 12.7 mmol) in 5 mL of DMF was refluxed with stirring for 8 h. The reaction mixture was cooled to room temperature and poured into 50 mL of ethyl acetate. The resulting mixture was sonicated for about 30 min to get precipitate. The obtained white colored amorphous solid was filtered off, washed with excess of ethyl acetate and dried at 40 °C for 10 h. Yield: 82%. M.p.: above 300 °C. ¹H NMR (400 MHz, CDCl₃) δ (ppm): 8.14–8.12 (m, 2H, Ar-H), 7.99–7.50 (m, 33H, Ar-H), 7.16–7.12 (m, 4H, Ar-H), 5.26 (s, 4H, Ar-CH₂), 4.13 (s, 3H, -O-CH₃), FTIR (ATR, cm⁻¹): 3365, 3051, 2853, 2211, 1658, 1430, 1103, 728, 682, 495. Element. Anal. Calc. For C₅₇H₄₆Br₂N₂O₂: C, 68.68; H, 4.65; N, 2.81. Found: C, 68.66; H, 4.68; N, 2.84% (Scheme 1).

2.3.5. Synthesis of 3,4-bis(tetradecyloxy)-N'2,N'5-bis-3-(thiophen-2-yl)acryloyl thiophene-2,5-dicarbohydrazide (**6**)

To a mixture of compound **5** (5 g, 8 mmol) and 2 mL of pyridine in 50 mL of NMP, 3-(thiophen-2-yl)acrylyl chloride (2.76 g, 16 mmol) was added slowly at room temperature while stirring. The stirring was continued at room temperature for 12 h. The reaction mixture was poured into excess of water to get a precipitate. The precipitate obtained was collected by filtration, washed with excess of water, dried in oven and re-crystallized from ethanol/chloroform mixture. Yield: 82%. M.p.: 210–212 °C. ¹H NMR (400 MHz, CDCl₃) δ (ppm): 9.98 (s, 2H, -CONH-), 9.21 (s, 2H, -CONH-), 7.74 (d, 2H, -CH=CH-, J = 16 Hz), 7.42 (d, 2H, Ar-H, J = 4.8 Hz), 7.29 (d, 2H, Ar-H, J = 3.6), 7.10 (m, 2H, Ar-H), 6.9 (d, 2H, -CH=CH-, J = 16 Hz), 4.31 (t, 4H, -O-CH₂-, J = 7 Hz), 1.24–1.83 (m, 48H, -(CH₂)₁₀-), 0.89 (t, 6H, Ar-CH₃, J = 6.8 Hz). FTIR (KBr, cm⁻¹): 3310, 3214, 2918, 2852, 1685, 1648, 1495, 1303, 1051, 931, 723. Element. Anal. Calc. For: C₄₈H₇₂N₄O₆S₃: C, 64.25; H, 8.09; N, 6.24; S, 10.72. Found: C, 64.27; H, 8.14; N, 6.29; S, 10.78%.

2.3.6. Synthesis of 5,5'-(3,4-bis(tetradecyloxy)thiophene-2,5-diyl)bis(2-(-2-(thiophen-2-yl) vinyl)-1,3,4-oxadiazole) (**7**)

A mixture of compound **6** (3 g, 3.4 mmol) and 50 mL of phosphorous oxychloride was heated at 80 °C for 6 h. The reaction mixture was then cooled to room temperature and poured into crushed ice. The resulting precipitate was collected by filtration, washed with water and dried in oven. Further purification was done by column chromatography using silica gel using PE/EA as eluent. Yield 56%, m.p.: 189–190 °C. ¹H NMR (400 MHz, CDCl₃) δ (ppm): 7.74 (d, 2H, -CH=CH-, J = 16 Hz), 7.42 (d, 2H, Ar-H, J = 4.8 Hz), 7.29 (d, 2H, Ar-H, J = 3.6), 7.10 (m, 2H, Ar-H), 6.9 (d, 2H, -CH=CH-, J = 16 Hz), 4.31 (t, 4H, -O-CH₂-, J = 7 Hz), 1.24–1.83 (m, 48H, -(CH₂)₁₀-), 0.89 (t, 6H, Ar-CH₃, J = 6.8 Hz). FTIR (KBr, cm⁻¹): 2916, 2849, 1585 (-C=N-), 1458, 1274, 1044, 955, 712. Element. Anal. Calc. For: C₄₈H₆₈N₄O₄S₃: C, 66.94; H,

7.96; N, 6.51; S, 11.17. Found: C, 67.00; H, 7.99; N, 6.55; S, 11.20%.

2.3.7. Synthesis of 2,2'-(5,5'-(3,4-bis(tetradecyloxy)thiophene-2,5-diyl)bis(1,3,4-oxadiazole-5,2-diyl)) bis(ethene-2,1-diyl)dithiophene-2-carbaldehyde (**8**)

Dialdehyde **8** was synthesized by using the Vilsmeier-Haack reaction. *N,N* Dimethylformamide (0.954 g, 13 mol) cooled to 0 °C was treated drop wise with phosphorus oxychloride (1.989 g, 13 mol). The resulting orange solution was stirred at 0 °C for 1 h and at 25 °C for 1 h, and then compound **7** (2 g, 2.18 mmol) in 20 mL of 1,2-dichloroethane was added slowly. The mixture was heated at 90 °C for 24 h, cooled, and poured onto 200 g of crushed ice. Brown oil separated, which was taken up in dichloromethane. The extract was washed with saturated aqueous bicarbonate and then with water containing a little ammonium chloride and the organic layer was dried over anhydrous Na₂SO₄. The solvent was removed under reduced pressure, and the crude viscous product was separated on a silica gel column, using hexane:ethyl acetate (1:1) as eluent. The yield of the dialdehyde was 37%. ¹H NMR (400 MHz, CDCl₃) δ (ppm): 9.94 (s, 2H, Ar-CHO), 7.74 (m, 4H, -CH=CH-), 7.37 (d, 2H, Ar-H, J = 4.8 Hz), 7.11 (m, 2H, Ar-H), 4.31 (t, 4H, -O-CH₂-, J = 7 Hz), 1.85–1.24 (m, 48H, -(CH₂)₁₀-), 0.87 (t, 6H, Ar-CH₃, J = 6.8 Hz). FTIR (KBr, cm⁻¹): 2918, 2849, 1662 (-HC=O), 1590, 1458, 1354, 1044, 809, 720. Element. Anal. Calc. For: C₅₀H₆₈N₄O₆S₃: C, 65.47; H, 7.47; N, 6.11; S, 10.49. Found: C 65.50; H, 7.54; N, 6.20; S, 10.51%.

2.3.8. Synthesis of polymers

2.3.8.1. General procedure for the synthesis of polyhydrazides PH1-PH3. To a stirred solution of monomer **5** (0.5 mmol as a representative) in *N*-methylpyrrolidinone (NMP) (20 mL) containing LiCl (0.1 g) and 1–2 drops of pyridine was added to another monomer diacid chloride. The reaction mixture was then heated to 80 °C and stirred at this temperature for 20 h. After cooling to room temperature, precipitation in CH₃OH and washing with water and ethanol afforded a high yield (90–95%) of a polyhydrazide.

PH1. ¹H NMR, (400 MHz, CDCl₃) δ (ppm): 10.99 (s, 1H, -CONH-), 9.89 (s, 1H, -CONH), 7.9–7.7 (m, 2H, Ar-H), 4.3–4.25 (m, 4H, -OCH₂-), 1.9–1.2 (m, -CH₂-, 48H), 0.840 (s, 6H-CH₂-CH₃). FTIR (KBr, v, cm⁻¹): 3299 (-NHCO-), 2919, 2851, 1633, 1457, 1289, 1041, 715.

PH2. ¹H NMR, (400 MHz, CDCl₃) δ (ppm): 10.9 (d, 1H, -CONH-), 9.8 (s, 1H, -CONH-), 7.90–7.45 (m, 6H, Ar-H), 4.21 (s, 4H, -OCH₂-), 1.23–1.89 (m, 48H, -CH₂-), 0.85 (t, 6H, -CH₂-CH₃). FTIR (KBr, v, cm⁻¹): 3266 (-N-H), 2920, 2852 (-C-H) 1633 (>C=O) 1460 (aromatic-CH-), 1037 (-C-O-C-).

PH3. ¹H NMR, (400 MHz, CDCl₃) δ (ppm): 11.17–11.03 (d, 1H, -CONH-), 10.00–9.96 (s, 1H, -CONH), 7.09–6.62 (m, 2H, Ar-H), 4.3–4.25 (m, 4H, -OCH₂-), 1.91–1.06 (m, -CH₂-, 48H), 0.843 (s, 6H, -CH₂-CH₃). FTIR (KBr, v, cm⁻¹): 3230 (-NHCO-), 2920, 2851, 1634, 1605, 1457, 1301, 1041, 727.

2.3.8.2. General procedure for the synthesis of polymers P1-P3. The precursor polyhydrazide **PH1-PH3**, (0.2 g) was dispersed in 20 mL of POCl₃ at room temperature. The mixture

was refluxed for 12 h. After cooling to room temperature, the reaction mixture was poured into water. The precipitate was collected by filtration and was washed with water, ethanol, followed by ether and finally dried under vacuum at room temperature. The yield was in the range 85–90%.

P1. ^1H NMR, (400 MHz, CDCl_3), δ (ppm):

P1. ^1H NMR, (400 MHz, CDCl_3), δ (ppm): 8.15–8.11(m 2H, Ar-H), 4.34–4.28 (m, 4H, $-\text{OCH}_2-$), 1.95–1.25 (m, $-\text{CH}_2-$, 48H), 0.890(s, 6H, $-\text{CH}_3$). FTIR (KBr, ν , cm^{-1}): 2921, 2853, 1575, 1461, 1368, 1283, 1030, 818, 725. Weight average molecular weight (M_w) is 13800 with poly dispersity (PDI) = 2.24.

P2. ^1H NMR, (400 MHz, CDCl_3), δ (ppm): 7.96–7.50 (m, 6H, Ar-H), 4.2(s, 4H, $-\text{OCH}_2\text{O}$), 1.2–1.9 (m, 48H), 0.86 (t, 6H). FTIR, (cm^{-1}): 2919–2851($-\text{C}-\text{H}$), 1582–1524 ($>\text{C}=\text{N}-$), 1459, 1368, 1038 ($-\text{C}-\text{O}-\text{C}-$). Weight average molecular weight (M_w) is 8300 with poly dispersity (PDI) = 2.35.

P3. ^1H NMR, (400 MHz, CDCl_3), δ (ppm): 7.15–7.58(m 2H, vinylic), 4.345 (m, 4H, $-\text{OCH}_2-$), 1.89–1.24 (m, $-\text{CH}_2-$, 48H), 0.849(s, 6H, $-\text{CH}_3$). FTIR (KBr, ν , cm^{-1}): 2919, 2851, 1576, 1460, 1371, 1290, 1007. Weight average molecular weight (M_w) is 15300 with poly dispersity (PDI) = 2.04.

2.3.8.3. General procedure for the synthesis of P4–P5. Compound **4** (0.5 mmol) and compound **8** (0.5 mmol) were dissolved in a mixture of 5 mL of chloroform and 15 mL of ethanol. Sodium ethoxide (0.030 g, 1 mmol in 10 mL of ethanol) was added to the reaction mass at room temperature under nitrogen atmosphere. Then, reaction mixture turned into yellow color. It was stirred for 12 h at room temperature. After the completion of the reaction, solvent was removed off under reduced pressure. Then the crude reaction mass was poured into excess of methanol and stirred for about 30 min. The obtained polymer was filtered and then washed thoroughly with acetone, re-dissolved in chloroform and poured into excess of methanol to remove oligomers. The resulting precipitate was filtered off and dried at 40 °C under vacuum for 24 h to give fluorescent deep greenish yellow colored powder. On the similar lines, polymer **P5** was prepared. The characterization data of **P4–P5** are given below.

P4: ^1H NMR, (400 MHz, CDCl_3), δ (ppm): 8.21–6.73 (m, 19 H, Ar-H, vinylic), 4.30–4.21(m, 7H), 2.17–1.24 (m, $-\text{CH}_2-$), 0.86 (s, $-\text{CH}_2-\text{CH}_3$). FTIR (KBr, cm^{-1}): 2919, 2849, 2218($-\text{CN}$), 1576, 1449, 1358, 1257, 1013, 947, 806. Weight average molecular weight (M_w) is 18200 with poly dispersity (PDI) = 2.5.

P5: ^1H NMR, (400 MHz, CDCl_3), δ (ppm): 7.75–7.26 (m, 14 H, Ar-H, vinylic), 4.42–4.25(m, 4H), 1.85–1.23 (m, $-\text{CH}_2-$), 0.86 (s, $-\text{CH}_2-\text{CH}_3$). FTIR (KBr, cm^{-1}): 2919, 2850, 2220(CN), 1625, 1582, 1455, 1364, 1073, 947. Weight average molecular weight (M_w): 27800 with Poly dispersity (PDI) = 4.

3. Results and discussion

3.1. Synthetic design

In the present article, five new donor acceptor type conjugated polymers **P1–P5** were synthesized through

polycondensation, Wittig, and Knoevenagel reactions. The polymers **P1–P3** were synthesized from dihydrazide monomer **5**, in which the dihydrazide monomer was made to react with corresponding diacidchlorides and then the resulting polyhydrazides were converted into polyoxadiazoles using phosphorus oxychloride as cycling agent.

The required chalcone **1** was prepared from toluadehyde and 4-methyl acetophenone using Claisen–Schmidt reaction. It was then cyclized to cyanopyridine **2** by reacting it with malononitrile in presence of sodium methoxide. Further, its methyl groups were brominated by Wholzigler method using NBS and BPO. The resulting dibromo derivative **3** was conveniently converted to phosphonium Wittig salt **4**, which on treatment with dialdehyde **8** in presence of ethanol-chloroform medium yielded final polymer **P4**. The same dialdehyde monomer **8** was made to react with 1,4-phenyldiacetonitrile via Knoevenagel condensation to yield the polymer **P5**.

3.2. Characterization

Structures of the intermediates as well as target polymers were established by elemental analysis and spectroscopic techniques. The spectral characteristics of chalcone **1** matched with the reported data. Cyclization of chalcone to cyano pyridine **2** was confirmed by its ^1H NMR spectrum wherein it showed a signal at δ 4.19 ppm which corresponds to protons of $-\text{OCH}_3$ group attached to the pyridine ring. In its FTIR spectrum, it displayed a sharp peak at 2217 cm^{-1} indicating the presence of cyano group. Formation of compound **3** was confirmed by its ^1H NMR spectrum, where it showed a signal at δ 4.81 ppm that corresponds to methylene protons, which is deshielded to a greater extent when compared to compound **2**. Formation of compound **6** was confirmed by FTIR and ^1H NMR spectroscopic technique. It showed intense band at 3310 and 1685 cm^{-1} indicates the presence of $-\text{NH}-$ and $>\text{C}=\text{O}$ groups, respectively. Further ^1H NMR spectrum of this compound showed peaks at δ 9.21 and δ 9.98 ppm indicating the formation of amide. Structure of compound **7** was confirmed by FTIR, ^1H NMR and mass spectral analysis, it showed strong absorption band at 1585 cm^{-1} indicates the formation of oxadiazole ring. ^1H NMR spectrum of the compound showed disappearance of amidic protons and it also showed deshielding of aromatic protons due to the formation of oxadiazole ring and it also showed two doublets at δ 7.74 and δ 6.90 ppm corresponding to vinylic protons with coupling constant $J = 16\text{ Hz}$. Mass spectral analysis showed the $M+1$ peak at 862 which corresponds to the molecular formula $\text{C}_{48}\text{H}_{68}\text{N}_4\text{O}_4\text{S}_3$. The formation of compound **8** was confirmed by FTIR, ^1H NMR spectral and elemental analyses. It showed strong absorption band at 1662 cm^{-1} indicates the presence of the aldehydic carbonyl group and it was confirmed by ^1H NMR and it showed a peak at δ 9.94 ppm and one of the aromatic protons on the thiophene ring also disappeared from δ 7.29 ppm which confirms the formylation on either side. Elemental analysis showed percentage of elements corresponding to the molecular formula $\text{C}_{50}\text{H}_{68}\text{N}_4\text{O}_6\text{S}_3$. Structures of the polymers were confirmed by their ^1H NMR and FTIR spectral data.

The synthesized polymers are soluble in common organic solvents such as chloroform, dichloromethane, tetrahydrofuran and dimethyl sulfoxide. Thermogravimetric analysis (TGA) reveals good thermal stability of the polymers up to 300 °C. The degradation temperatures of the polymers were found to be 300, 304, 285, 321 and 310 °C for polymers **P1**, **P2**, **P3**, **P4** and **P5**, respectively. The gradual weight loss beyond 300 °C may be attributed to the degradation of the attached alkoxy chains on the thiophene rings. Similar behavior was observed for substituted polythiophenes in earlier reports. The weight loss that took place in the temperature range of ca. 300–900 °C corresponds to the degradation of polymer backbone leaving behind a residue content of less than 25%. Further, at higher temperature of TGA scan, there may be occurrence of cross-linking in polymer across longer side chain or degradation of side chains [16–18]. The molecular weights of the polymers were estimated by gel permeation chromatography using polystyrene standard. Weight average molecular weight (M_w) of these polymers were found to be 13800, 15300, 8300, 18200, 27800 with polydispersity (PDI) 2.24, 2.04, 2.35, 2.51 and 4.00, for polymers **P1**, **P2**, **P3**, **P4** and **P5**, respectively.

3.3. Linear optical properties

Optical properties of the polymers were studied by UV–Vis and fluorescence spectroscopic techniques. The UV–Vis absorption and fluorescence emission spectra were recorded in dilute THF (10^{-6} M) solutions. The absorption maxima of the polymers in dilute solutions were assignable to the π – π^* transition resulting from the conjugation between the aromatic rings and nitrogen atoms.

It has been also observed that the polymer showed higher absorption maxima when compared to other reported D–A type conjugated polymers derived from oxadiazole–thiophene systems. This is mainly due to introduction of various electron donating moieties such as naphthyl, thienyl, and vinylenyl units along the polymer backbone which results in increase in conjugation and reduction in steric hindrance of the bulky alkoxy side chains [19]. The UV–Vis and fluorescence spectra of the polymers in dilute solution are shown in Figs. 1 and 2. The Fig. 3 shows the fluorescence emission behavior of **P1**–**P5** in THF under UV irradiation. The quantum yields for emission in solution was determined according to the method described by Davey et al. (1992) [20,21] relative to quinine sulfate in 0.1 M H_2SO_4 . Polymers **P1**–**P5** were found to be strongly emissive with good quantum yields. This could be attributable to the rigid structure of the polymer with the effect that relaxation from the excited state through non-radiative (e.g., thermal) processes would be reduced with good fluorescence quantum yield [22]. The UV absorption and fluorescence emission spectra of the polymers are given in Table 1.

Absorption maxima of the polymer **P1**–**P3** altered by the variation of electron donating moiety as well as conjugation path length. In **P1** thiophene was used as electron donating moiety which is stronger donating moiety than that of naphthyl and vinylenyl moiety, due to this **P1** showed highest absorption maxima as well as emission

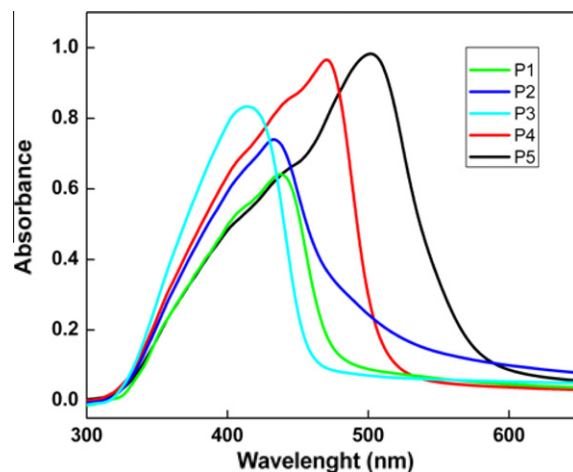


Fig. 1. UV–Vis absorption spectra of the polymer **P1**–**P5** in dilute solution.

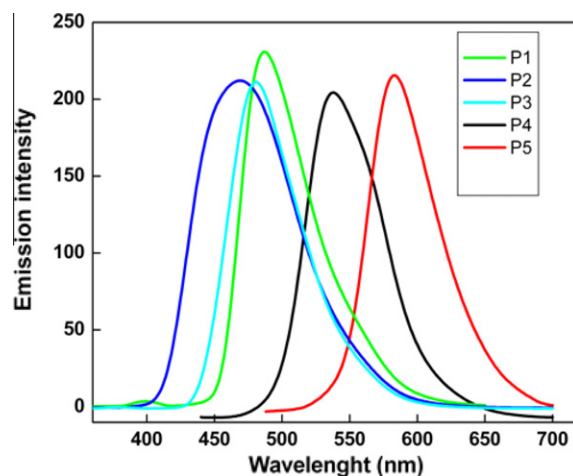


Fig. 2. Fluorescence studies of polymer **P1**–**P5** in THF solutions.

maxima amongst **P1**–**P3**. Similarly, in polymer **P4** we introduced cyanopyridine as another electron accepting moiety along the conjugation path length. Introduction of this led to the enhancement in the conjugation path length that resulted in increase in absorption maxima of **P4**. Furthermore, the presence of nitrile functional group increased its fluorescence nature. Similarly, when cyanovinylene units were incorporated in **P5**, large enhancement in absorption maxima as well as reduction in band gap were observed. The results of UV–Vis absorption studies indicate that, as donor and acceptor strengths increase in the polymer backbone, there is significant enhancement in the absorption maxima which leads to decrease in band gap of the resulting polymer. Because of this, the new polymers can be potential candidates for their applications in optoelectronic devices.

Stoke shift is another important parameter of a molecule for its use in various device applications. It occurs when emission from the lowest vibrational excited state relaxes to various vibrational levels of the electronic

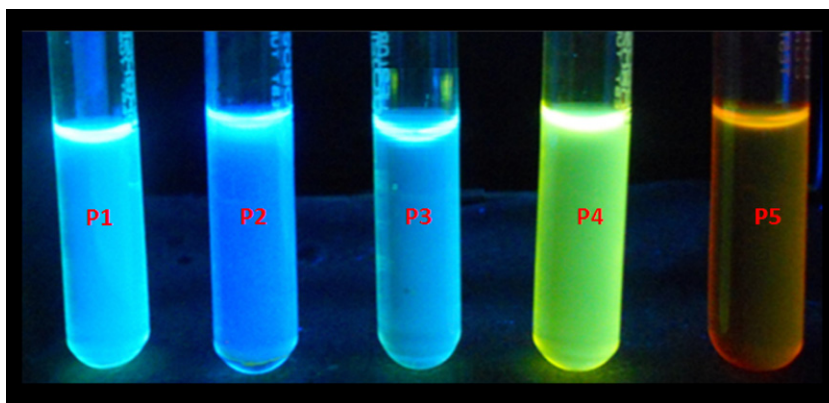


Fig. 3. Fluorescence emission in polymers under UV irradiation.

Table 1
Optical characterization data of polymers **P1–P5**.

Polymer UV	Absorption maxima in THF (nm)	Fluorescence emission maxima (nm)	Fluorescence Quantum yield (%)	$E(A_{\max})$ (eV)	$E(PL_{\max})$ (eV)	Stoke shift (eV)
P1	437	487	38	2.83	2.54	0.29
P2	433	468	35	2.86	2.65	0.21
P3	413	480	32	3.00	2.58	0.42
P4	471	538	44	2.63	2.30	0.33
P5	502	582	42	2.47	2.13	0.34

A_{\max} = Absorption maxima, PL_{\max} = Emission maxima.

ground state. The stoke shift of polymers **P1–P5** was calculated using the UV–Vis absorption maxima and fluorescence emission maxima recorded in the dilute THF solutions (10^{-6} M). The calculated values were found to be 0.29, 0.21, 0.42, 0.33 and 0.34 eV for **P1**, **P2**, **P3**, **P4** and **P5**, respectively. The results indicate that the polymers showed moderate stoke shifts when compared to the D-A type polymers reported in literature. Out of the studied polymers, **P3** showed maximum stoke shift of 0.42 eV, which may be attributed to the presence of less bulkier vinylic linkages. The polymer **P2** showed low Stoke shift value which may be ascribed to the presence of the bulky naphthalene unit along the polymeric backbone whereas polymers **P4** and **P5** showed a good stoke shift which may be due to the incorporation of cyanopyridine and cyanovinylene linkages, respectively. From the results, it can be concluded that the new polymers are good candidates for Stokes shift applications, such as high energy lasers, molecular imaging, scintillators, solar collectors and light emitting materials.

3.4. Electrochemical studies

Cyclic voltammetry (CV) was employed to determine redox potentials of newly synthesized polymers and then to estimate the HOMO and LUMO levels, which is of importance to determine the band gap. The cyclic voltammogram of the polymer coated on a glassy carbon electrode was obtained by AUTOLAB PGSTAT-30 electrochemical analyzer, using a Pt counter electrode and a Ag/AgCl reference

electrode, immersed in the electrolyte [0.1 M(n-Bu)₄N⁺(ClO₄)-inacetonitrile] at a scan rate of 25 mV/S [23].

All the measurements were calibrated using ferrocene as standard [24]. As shown in Fig. 4, the newly synthesized polymers were electro-active either in the cathodic region or in the anodic region. Oxidation and reduction potentials were estimated from cyclic voltammogram and they are summarized in Table 2. This *p*-doping and *n*-doping potential are comparable to other oxadiazole-containing light-emitting polymers [25] in the literature. The onset oxidation and reduction potentials were used to estimate the highest occupied molecular orbital (HOMO) and lowest unoccupied molecular orbital (LUMO) energy levels of the polymers. The equations, $E_{\text{HOMO}} = - [E_{\text{onset}}^{\text{oxd}} + 4.4 \text{ eV}]$ and $E_{\text{LUMO}} = - [E_{\text{onset}}^{\text{red}} - 4.4 \text{ eV}]$, where $E_{\text{onset}}^{\text{oxd}}$ and $E_{\text{onset}}^{\text{red}}$ are the onset potentials versus standard calomel electrode (SCE) for the oxidation and reduction of the material referred, were used for the calculation.

The observed electrochemical behavior in **P1–P5** can be well explained on the basis of their structure–property relationship. In general, when electron-withdrawing substituents (oxadiazoles) are attached to the conjugated molecules, the electron density in the π -system of the conjugated molecule will be decreased. Consequently, the molecule will be stabilized and its oxidation potential will be increased. This results in a shift of the HOMO energy level to lower energy. Similarly, presence of thiophene, naphthalene, and vinylene units influences significantly the HOMO energy level due to their high electron donating ability. Usually, the band gap of any conjugated polymer can be

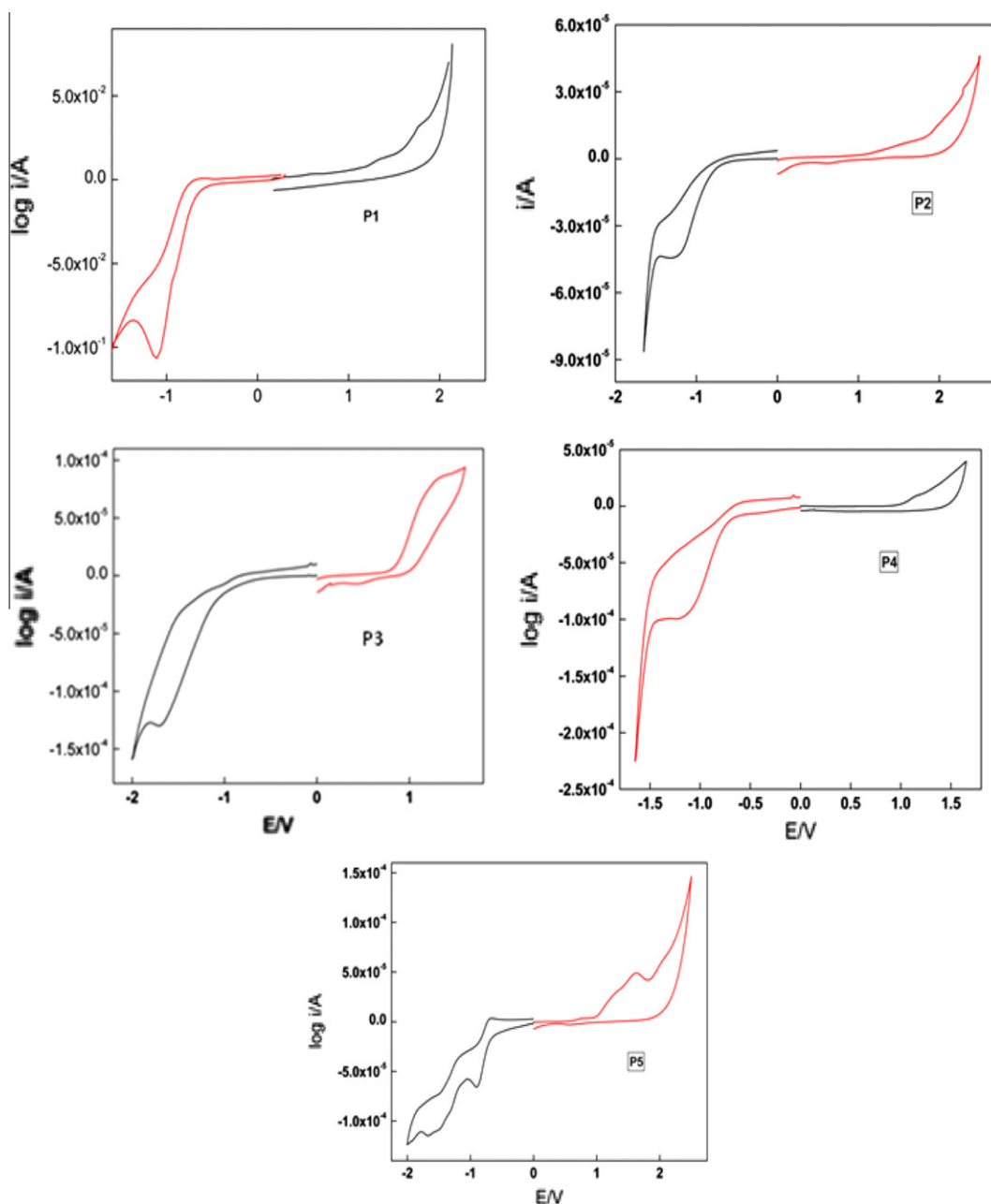


Fig. 4. Cyclic voltametric traces of P1–P5.

influenced by conjugation length, solid-state intermolecular ordering and the presence of electron-withdrawing or donating moieties. By varying these properties, optical and electrochemical behavior of such polymers can be tuned. The effective conjugation length, which is dependent upon the torsion angle between the repeating units along the polymer backbone, can be controlled by introduction of sterically hindered bulky dialkoxy side chains in order to twist the units out of plane. In polymers P1–P3, introduction of electron releasing thiophene, naphthalene and vinylene moieties in between 3,4-ditetradecyloxythiophene and

Table 2
Electrochemical characterization data of P1–P5.

Polymers	E_{oxd} (eV)	E_{red} (eV)	E_{oxd} (onset)	E_{red} (onset)	E_{HOMO} (eV)	E_{LUMO} (eV)	E_{g} (eV)
P1	1.77	-1.11	1.22	-0.68	-5.62	-3.72	1.9
P2	2.01	-1.25	1.22	-0.85	-5.62	-3.55	2.07
P3	1.31	-1.7	0.94	-1.14	-5.34	-3.26	2.08
P4	1.14	-1.18	0.99	-0.76	-5.39	-3.67	1.75
P5	1.64	-0.9	1.04	-0.68	-5.44	-3.72	1.72

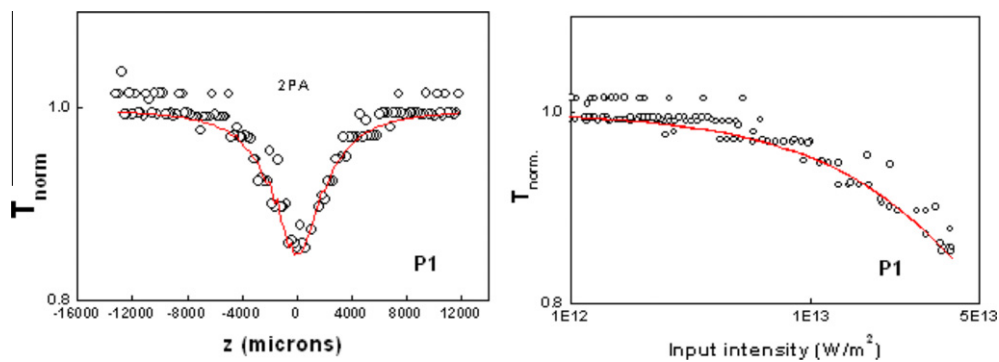


Fig. 5. Z-scan and fluence curve of **P1**.

oxadiazole units resulted in reduction in their band gap. In addition, incorporation of cyanopyridine moiety along the polymer **P4** decreased the band gap further due to the high electron withdrawing nature of the pyridine ring. Similarly, **P5** showed the lowest band gap in this series which is mainly attributed to the presence of highly electron withdrawing cyanovinylene units. Electrochemical potentials and energy levels of the polymers are tabulated in Table 2.

3.5. Third order nonlinear optical activity

3.5.1. Z-scan studies

A very convenient and fast experimental method to assess materials for NLO (including optical limiting) is the z-scan experiment [26]. This measure the magnitude of both the nonlinear refraction (NLR) and nonlinear absorption (NLA) as a function of incident laser intensity while the sample is gradually moved through the focus of a lens (along the z-axis). In the experiment, the sample is placed in the path of intense laser beam at different positions with respect to the focus (different values of z), and the corresponding transmission is measured. Then the sample exposes to different laser intensity at each position, and therefore its position-dependent transmission will give information on its intensity-dependent transmission as well. The effective nonlinear absorption coefficients were calculated by fitting theory. We used a stepper-motor-controlled linear translation stage in our setup to move the sample through the beam in precise steps. The sample was placed in a 1 mm cuvette. The transmission of the sample at each point was measured using two pyroelectric energy probes (Rj7620, Laser Probe Inc., Utica, NY, USA). One energy probe monitored the input energy while the other monitored the energy transmitted through the sample. The second harmonic output (532 nm) of a Q-switched Nd:YAG laser (Quanta Ray, Spectra Physics) was used to excite the molecules. The temporal width (FWHM) of the laser pulses was 7 ns. The pulses were fired in the “single shot” mode, allowing sufficient time between successive pulses to avoid accumulative thermal effects in the sample.

Fig. 5 shows the open aperture z-scan curves of the polymer **P1** in THF solution. In each polymers we have observed two photon absorption (TPA). The nonlinear activity of the polymer can be explained by considering pulse duration, pump intensity and wavelength. It can be explained by the transitions (a) ground state S_0 to higher excited singlet

states S_n (two-photon or multi-photon excitation) (b) the first excited singlet state S_1 to higher excited states S_n , and (c) the T_1 to T_n states in the triplet manifold. The last two processes are known as excited state absorption (ESA), and if their cross-sections are larger than that of the ground state linear absorption, then these are referred to as reverse saturable absorption (RSA). The net effect is then known as an “effective” TPA process.

The nonlinear transmission behavior of the present sample can therefore be modeled by defining an effective nonlinear absorption coefficient $\alpha(I)$, given by

$$\alpha(I) = \frac{\alpha_0}{1 + \left(\frac{I}{I_s}\right)} + \beta I \quad (1)$$

where α_0 is the unsaturated linear absorption coefficient at the wavelength of excitation, and I_s is the saturation intensity (intensity at which the linear absorption drops to half its original value). β is the effective TPA coefficient. For calculating the output laser intensity for a given input intensity, first we numerically evaluate the output intensity from the sample for each input intensity by solving the propagation equation,

$$\frac{dI}{dz} = - \left[\left(\alpha_0 / \left(1 + \frac{I}{I_s} \right) \right) + \beta I \right] I \quad (2)$$

using the fourth order Runge–Kutta method. Input intensities for the Gaussian laser beam for each sample position in the z-scan are calculated from the input energy, laser pulse width and irradiation area. Here ‘z’ indicates the propagation distance within the sample. The normalized transmittance is then calculated by dividing the output intensity with the input intensity and normalizing it with the linear transmittance.

Fig. 5 represents the open aperture Z-scan trace and fluence curve of the polymer **P1** (Z-scan and fluence curves of polymers **P2–P5** are given in the Supplementary information). As seen from Fig. 5, there is good agreement between the experimental data and numerical simulation. The numerically estimated values the effective TPA coefficients are 1.81×10^{-11} , 1.1×10^{-11} , 0.52×10^{-11} , 2.1×10^{-11} and 0.91×10^{-11} m/W, for polymers **P1**, **P2**, **P3**, **P4** and **P5**, respectively (Table 3). For comparison, under similar excitation conditions, NLO materials like Cu nanocomposite glasses showed effective TPA coefficient values of 10^{-10} – 10^{-12} m/W [27], functionalized carbon nanotubes

Table 3
Two-photon absorption coefficients of **P1–P5**.

Sl. No.	Polymers	Two-photon absorption coefficient (β) in m/W
1	P1	1.81×10^{-11}
2	P2	1.10×10^{-11}
3	P3	0.52×10^{-11}
4	P4	2.10×10^{-11}
5	P5	0.91×10^{-11}

showed 3×10^{-11} m/W [28], Bismuth nanorods gave 5.3×10^{-11} m/W [29], and CdS quantum dots exhibited 1.9×10^{-9} m/W [30]. Similarly, many π -conjugated polymers were shown to possess good two-photon absorption coefficients [31–33], of the order of 10^{-11} m/W with comparable optical limiting behavior. The observed TPA values for **P1–P5** demonstrate that the present samples exhibit optical nonlinear property comparable to those of good optical limiters reported in the literature, and are therefore potentially suitable for applications in optical limiting devices.

The improved nonlinear optical limiting behavior of **P1–P5** can be explained on the basis of their structures. Amongst **P1–P3**, polymer **P1** showed maximum optical limiting behavior which is attributed to introduction of electron releasing thiophene ring system in between alkoxythiophene and oxadiazole rings. Interestingly, polymer **P4** displayed maximum TPA coefficient among five polymers. This observed fact is mainly due to introduction of highly electron-withdrawing cyanopyridine unit along the polymer backbone. The presence of this cyanopyridine in between the vinylene units enhanced the D–A nature of the polymer as well as conjugation path length. This enhancement in the conjugation led to increase in the molecular hyperpolarizability which in turn enhanced the optical limiting behavior of the resulting polymer.

4. Conclusion

Five new D–A type thiophene based conjugated polymers, **P1–P5**, carrying highly electron releasing ditetradecyloxythiophene, naphthalene and vinylene units, and strong electron withdrawing oxadiazole, cyanopyridine and cyanovinylene moieties were successfully synthesized and characterized using various techniques. The results of the linear optical properties revealed that absorption maxima and emission maxima of the polymers can be enhanced by increasing donor strength and conjugation path length. From the results of optical limiting properties of these polymers it can be concluded that the optical nonlinearity also depends on the extent of conjugation path length and D–A nature prevailing the polymer chain. Amongst five polymers, **P4** showed strong optical limiting behavior with the highest two photon absorption coefficient of 2.1×10^{-11} m/W. The study reveals that these new polymers are promising materials for the development of efficient photonic devices.

Acknowledgements

The authors are grateful to NITK Surathkal, RRI, Bangalore, CDRI, Lucknow, IISc, Bangalore, STIC Cochin and SAIF Gujarat for providing instrumental analyses.

Appendix A. Supplementary data

Supplementary data associated with this article can be found, in the online version, at <http://dx.doi.org/10.1016/j.eurpolymj.2012.06.003>.

References

- [1] Tutt LW, Kost A. Optical limiting performance of C60 and C70 solutions. *Nature* 1992;356:225–6.
- [2] Tutt LW, Boggess TF. A review of optical limiting mechanisms and devices using organics, fullerenes, semiconductors and other materials. *Prog Quant Electron* 1993;17(4):299–338.
- [3] Batista RMF, Costa SPG, Belsley M, Raposo MM. Synthesis and second-order nonlinear optical properties of new chromophores containing benzimidazole, thiophene, and pyrrole heterocycles. *Tetrahedron* 2007;63:9842–9.
- [4] Hao J, Han MJ, Guo K, Zhao Y, Qiu L, Shen Y, et al. A novel NLO azothiophene-based chromophore: Synthesis, characterization, thermal stability and optical nonlinearity. *Mater Lett* 2008;62(6–7):973–6.
- [5] Cassano T, Tommasi R, Babudri F. High third-order nonlinear optical susceptibility in new fluorinated poly(*p*-phenylenevinylene) copolymers measured with the Z-scan technique. *Opt Lett* 2002;27:2176–2178.
- [6] Udayakumar D, Adhikari AV. Synthesis and characterization of new light-emitting copolymers containing 3,4-dialkoxythiophenes. *Synth Met* 2006;156:1168–73.
- [7] Udayakumar D, Adhikari AV. Synthesis and characterization of fluorescent poly(oxadiazole)s containing 3,4-dialkoxythiophenes. *Opt Mater* 2007;29:1710–8.
- [8] Hongli W, Zhen L, Bin H, Zuoquan J, Yanke L, Hui W, et al. Synthesis, light-emitting and optical limiting properties of new donor-acceptor conjugated polymers derived from 3,5-dicyano-2,4,6-tristyrylpyridine. *React Funct Polym* 2006;66:993–1002.
- [9] Michelle S, Liu X, Jiang, Sen L, Petra H, Alex KYJ. Effect of cyano substituents on electron affinity and electron-transporting properties of conjugated polymers. *Macromolecules* 2002;35(9):3532–8.
- [10] Sun WF, Byeon CC, Mckerns MM, Lawson CM, Gray GM, Wang DY. Optical limiting performances of asymmetric pentaazadentate porphyrin-like cadmium complexes. *Appl Phys Lett* 1998;73:1167–1169.
- [11] Wang P, Ming H, Xie JP, Zhang WJ, Gao XM, Xu Z. Substituents effect on the nonlinear optical properties of C60 derivatives. *Opt Commun* 2001;192(3–6):387–91.
- [12] Qu SL, Song YL, Du CM, Wang YX, Gao YC, Liu ST. Nonlinear optical properties in three novel nanocomposites with gold nanoparticles. *Opt Commun* 2001;196:317–23.
- [13] Zhou GJ, Zhang S, Wu PJ, Ye C. Optical limiting properties of soluble poly(thienyleneethynylene)s. *Chem Phys Lett* 2002;363(5–6):610–4.
- [14] Sun WF, Wu ZX, Yang QZ, Wu LZ, Tung CH. Reverse saturable absorption of platinum ter/bipyridyl polyphenylacetylide complexes. *Appl Phys Lett* 2003;82:850–2.
- [15] Sun WF, Bader MM, Carvalho T. Third-order optical nonlinearities of α , ω -dithienylpolyenes and oligo(thienylvinylene). *Opt Commun* 2003;215:185.
- [16] Hu X, Xu L. Structure and properties of 3-alkoxy substituted polythiophene synthesized at low temperature. *Polymer* 2000;41:9147–9154.
- [17] Swager TM, Gil CJ, Wrighton MS. Fluorescence studies of poly(*p*-phenyleneethynylene)s: the effect of anthracene substitution. *J Phys Chem* 1995;99:4886–93.
- [18] Marcos RAA, Hallen DR, Calado CL, Donnici TM. Synthesis and characterization of new 3-substituted thiophene copolymers. *J Braz Chem Soc* 2011;22(2):248–56.
- [19] Bin Z, Daxi L, Li P, Hui L, Ping S, Na Xiang, Yijiang L, Songting T. Effect of oxadiazole side chains based on alternating fluorene-thiophene copolymers for photovoltaic cells. *Eur Polym J* 2009;45:2079–2086.
- [20] Mikroyannidis JA, Damouras PA, Maragos VG, Tsai LR, Chen Y. Synthesis, photophysics and electroluminescence of new vinylene-copolymers with 2,4,6-triphenylpyridine kinked segments along the main chain. *Eur Polym J* 2009;45:284–94.
- [21] Davey AP, Elliott, Connor O, Blau W. New rigid backbone conjugated organic polymers with large fluorescence quantum yields. *J Chem Soc, Chem Commun* 1995;1433–1434.
- [22] Kang TJ, Jae YK, Kyung JK, Changjin L, Suh BR. Photoluminescence properties of various polythiophene derivatives. *Synth Met* 1995;69(1–3):377–8.

- [23] Sun Q, Wang H, Yang C, Li Y. Synthesis and electroluminescence of novel copolymers containing crown ether spacers. *J Mater Chem* 2003;13:800–6.
- [24] Pommerehe J, Vestweber H, Guss W, Mahrt RF, Bassler H, Porsch M, et al. Efficient two layer leds on a polymer blend basis. *Adv Mater* 1995;7:551–4.
- [25] Strukelji M, Papadimitrakoulous F, Miller TM, Rothberg LJ. Design and application of electron-transporting organic materials. *Science* 1995;267:1969–72.
- [26] Sheik-Bahae M, Said AA, Wei T. Sensitive measurement of optical nonlinearities using a single beam. *IEEE J Quantum Electron* 1990;26:760–9.
- [27] Karthikeyan B, Anija M, Sandeep SCS, Nadeer MTM, Philip R. Optical and nonlinear optical properties of copper nanocomposite glasses annealed near the glass softening temperature. *Opt Commun* 2008;281(10):2933–7.
- [28] Nan H, Yu C, Jinrui B, Jun W, Werner JB, Jinhui Z. Preparation and optical limiting properties of multiwalled carbon nanotubes with π -conjugated metal-free phthalocyanine moieties. *Phys Chem C* 2009;113(30):13029–35.
- [29] Sivaramakrishnan S, Muthukumar VS, Sivasankara S, Venkataramanaiah SK, Reppert J, Rao AM, et al. Nonlinear optical scattering and absorption in bismuth nanorod suspensions. *Appl Phys Lett* 2007;91:093104–7.
- [30] Kurian PA, Vijayan C, Sathiyamoorthy K, Suchand Sandeep CS, Reji P. *Nano Res Lett* 2007;2:561–567.
- [31] Samoc M, Samoc A, Davies BL. Two-photon and one-photon resonant third-order nonlinear optical properties of π -conjugated polymers. *Synth Met* 2000;109:79–83.
- [32] Qian Y, Meng K, Lu CG, Lin B, Huan W, Cui Y. The synthesis photophysical properties and two-photon absorption of triphenylamine multi-polar chromophores. *Dyes Pigm* 2009;80:174–180.
- [33] Hu JL, Li B, Meng FS, Ding F, Qian SX, Tian H. Two-photon absorption properties of hyper-branched conjugated polymers with triphenylamine as the core. *Polymer* 2004;45:7143–9.